Applied Catalysis A: General 493 (2015) 142–148

Contents lists available at ScienceDirect

Applied Catalysis A: General

journal homepage: www.elsevier.com/locate/apcata

Phosphoric acid intercalated Mg–Al hydrotalcite-like compounds for catalytic carboxylation reaction of methanol in a continuous system

Salwa Bougacha Ghorbel[a,*], Francisco Medina[b,c,**], Abdelhamid Ghorbel[a], Anna M. Segarra[b,c,**]

[a] Laboratoire de Chimie des Matériaux et de Catalyse, Faculté des sciences de Tunis, Université de Tunis El Manar, 2092, Tunisia
[b] Departament d'Enginyeria Química, Universitat Rovira i Virgili, 43007 Tarragona, Spain
[c] EMaS-Research Center on Engineering of Materials and Micro/nano Systems, University Rovira I Virgili, Marcel·lí Domingo, s/n, 43007 Tarragona, Spain

ARTICLE INFO

Article history:
Received 9 July 2014
Received in revised form
19 December 2014
Accepted 5 January 2015
Available online 13 January 2015

Keywords:
Mg–Al layered double hydroxides
Phosphate species
^{27}Al MAS NMR
^{31}P MAS NMR
TPD
SEM
Carboxylation reaction
Dimethyl carbonate
Acid–base bifunctional catalyst

ABSTRACT

Mg–Al-hydrotalcite-like catalysts (HTlcs) with different amount of P/Mg molar ratio were prepared via co-precipitation method and calcined at 450 °C. The synthesized catalysts were tested in the direct-carboxylation reaction of methanol in gas phase in a continuous system such as chemical route for CO_2 valorization. Activities around 2% with total selectivity towards the dimethyl carbonate (DMC) was obtained at moderate temperatures (150 °C) with both Mg/Al mixed oxides (HTO) and phosphated Mg/Al mixed oxides (HT*c*-9c). Even though the conversion increased until 16% at higher temperatures (200 °C), the selectivity with both catalysts (HTO and HT*c*-9c) decreased due to the decomposition of DMC to dimethyl ether (DME). Nevertheless, the catalyst with P showed less DMC decomposition and a higher selectivity towards the desired product. This is explained by the presence of orthophosphate species bonded to the Al^{3+} metals of the HTs ($O{=}P(OAl)_3$) which give to the catalyst a higher structural stability and specific acid properties.

In addition, the solids were characterized in-depth by XRD, ICP, NH_3-TPD, FTIR, Raman, ^{27}Al and ^{31}P MAS NMR spectroscopy and SEM.

1. Introduction

Hydrotalcite-like compounds (HTlcs) are layered double hydroxides (LDHs) also known as anionic clays and have the general formula $[M^{2+}_{1-x}M^{3+}_{x}(OH)_2]^{x+}[A^{n-}]_{x/n}\cdot yH_2O$, where M^{2+} and M^{3+} are di- and tri-valent metal cations, respectively, A^{n-} is a charge-balancing anion, and x is the molar ratio $M^{3+}/(M^{3+}+M^{2+})$ ranging from 0.1 to 0.5. Although, the x ratio of a pure hydrotalcite phase ranges from 0.17 to 0.33 [1]. The structure consists of brucite-like layers $[Mg(OH)_2]$ with an edge-sharing hydroxyl octahedral occupied by metal M^{2+} Some di-valent cations in hydrotalcites are isomorphically substituted by tri-valent ones. The positive charge generated on the layers is balanced by anions located in the interlayer alongside water molecules. Hydrotalcites are usually prepared by co-precipitation from metal salts in alkaline media at constant pH followed by a hydrothermal treatment of the precipitate. The usual activation protocol for these materials is a controlled thermal decomposition that leads to the formation of mixed oxides with a good dispersion of metals, a large specific surface area and Lewis basic properties. The rehydration of calcined hydrotalcite under a CO_2 free atmosphere allows the recovery of a layered structure that interlayer anions made of OH^- and therefore very good Brønsted basic properties [2].

The literature shows the capacity of hydrotalcite-like compounds to adsorb or intercalate phosphates and phosphoric acid derivates. For example, Hayashi et al. were able to synthesize Al–Mg hydrotalcites with intercalated phosphate ions from Cl-intercalated Al–Mg hydrotalcites due to the large ion-exchange capacity of hydrotalcites [3,4]. Parida et al. studied the ability of Cl-intercalated Mg–Al hydrotalcites to adsorb phosphates. They concluded that these hydrotalcites can be used as an effective adsorbent for removing phosphates from aqueous solutions with a maximum loading capacity of 44 mg of phosphate/g HTlcs and that the competing anions in solution had a strong effect on phosphate

---

[*] Corresponding author. Tel.: +216 71872600; fax: +216 71871666.
[**] Corresponding authors at: Departament d'Enginyeria Química, Universitat Rovira i Virgili, 43007 Tarragona, Spain; EMaS-Research Center on Engineering of Materials and Micro/nano Systems, University Rovira I Virgili, Marcel·lí Domingo, s/n, 43007 Tarragona, Spain.
E-mail address: Salwa.bougacha@fst.rnu.tn (S. Bougacha Ghorbel).

http://dx.doi.org/10.1016/j.apcata.2015.01.004
0926-860X/

adsorption [5]. Calcinating the hydrotalcite-like compound also increased its phosphate adsorption capacity. This is attributed to the following physicochemical properties of the calcined hydrotalcite: (i) the memory effect of the hydrotalcite layers, which allow phosphates to be incorporated as an interlayer anion, (ii) the greater surface area, which allows higher surface adsorption of the phosphates, and (iii) the elimination of the interlayer carbonate, which is the major obstacle to the incorporation of the phosphates as an interlayer anion [6]. Recently, Parida et al. have prepared new materials based on molybdophosphoric and tungstophosphoric acid intercalated in Zr/Al-hydrotalcite-like compounds by co-precipitation using an indirect method based on the terephthalic acid intercalated Zr/Al hydrotalcite as precursor [7].

The synthesis of dimethyl carbonate (DMC) by carboxylation reaction is a very interesting catalytic process since DMC is a safe, non-corrosive, and environmentally acceptable alternative to methylating and carbonylating agents [8]. Nowadays, industrial scale DMC synthesis is based on the oxidative carbonylation of MeOH by means of phosgene-free technologies. However, the reactant mixture used in this process is highly flammable and toxic; consequently, DMC synthesis using CO_2 represents an eco-friendly and economic alternative. Moreover, DMC has been proposed for use as an octane booster in gasoline and as an additive to diesel fuel to decrease particulate matter emissions [9].

The advantages of heterogeneous catalysts over their homogeneous counterparts mean they are preferred by the chemical industry [9]. Recently, it has been reported that DMC can be synthesized selectively and directly from CH_3OH and CO_2 in the presence of CeO_2 [10] and ZrO_2 [11] as heterogeneous catalysts in a batch reactor with a conversion of around 1%. The results of the catalyst characterization suggest that the acid–base bifunction is an important factor for a selective DMC synthesis. In this context, the LDH materials, especially Mg(Al)O mixed oxides, are potential candidates for use as successful heterogeneous catalysts in this reaction.

Developing a more active direct heterogeneous reaction between CO_2 and the alcohols MeOH and EtOH in order to synthesize the carbonic acid diesters dimethyl carbonate or diethyl carbonate (DEC) (Eq. (1)) is a very attractive prospect in terms of CO_2 chemical fixation and green chemistry, and may also help to further the substitution of phosgene for CO_2 [12]. Therefore, it is worthwhile exploring new ways to valorize CO_2 by generating fine chemicals such as carbonates.

$$2ROH + CO_2 \leftrightarrows (RO)_2CO + H_2O \quad (R = Me, Et) \tag{1}$$

The keys for achieving this aim are the design and development of an efficient process with a success catalyst. For the catalyst, the challenge remains to develop easy, environmentally friendly and versatile methods for the synthesis of layered double hydrotalcites with tuneable morphology, textures, chemical compositions and desirable acid and basic properties. Furthermore, obtaining an in-depth characterization and understanding of the properties of phosphate intercalated HTlcs is critical for their practical use as catalysts and it will help to avoid the trial-and-error practice. On the other hand, the process design should facilitate displacing equilibrium to DMC.

In this context, the current study describes the synthesis by co-precipitation of hierarchical Mg–Al HTlcs containing phosphates. The solids were characterized by NH_3 TPD, elemental analysis and Raman, IR and NMR spectroscopies. Furthermore, to the best of our knowledgement, the present work also describes for the first time the use of hydrotalcite-like materials as heterogeneous catalyst in the carboxylation reaction of methanol using a continuous reactor. The preliminary results obtained in this work have slightly improved with respect to the described in the literature. In addition, they are in the direction of designing more-efficient heterogeneous catalysts and reaction systems for CO_2 valorization as a potential source of economic and environmental benefits for the industry and the society.

2. Experimental

2.1. Catalyst preparation

All chemicals used for synthesis were purchased from Fluka or Merck.

The hydrotalcite-like materials were obtained by the co-precipitation method, which involved either the simultaneous addition of de-carbonated $MgCl_2·6H_2O$ and $AlCl_3·9H_2O$ solutions (Table 1, entries 1–6); or $Mg(NO_3)_2·6H_2O$ and $Al(NO_3)_3·9H_2O$ (Table 1, entries 7–9) in a molar ratio of $Al/(Al + Mg) = 0.25$. The pH was controlled by the simultaneous addition of 2 M NaOH solution. Both solutions were mixed under vigorous stirring. A 0.1 M Na_2HPO_4 solution was added during the synthesis to incorporate the phosphates species in the interlayer space of the HTlc materials. The reactants were added under inert atmosphere to prevent carbonate species from entering the interlayer space of the HTlcs. After the precipitation, the resulting gel was maintained under a vigorous agitation at 80 °C for 18 h. The precipitated solid was filtered and washed several times with decarbonated water to remove the excess ions and dried at 100 °C to yield the different materials. The experimental conditions for the synthesis of the different samples are presented in Table 1.

2.2. Catalyst characterization

The crystallographic characterization of the different samples was performed by X-ray powder diffraction (XRD). Diffraction patterns of intensity versus two theta (2θ) were recorded with a Phillips XRD 1050/70 X-ray diffractometer using Cu Kα radiation ($\lambda = 1.5418$ Å). Mg, Al, Cl and P analyses were performed by inductive coupled plasma (ICP) using a Perkin Elmer 3300 instrument. The carbon analysis was performed using a Bernard Calcimeter. The presence of nitrate ions was determined by ionic chromatography of the NE-ENIS 10304-1-1995 type.

FTIR spectra of the samples were recorded in a Perkin Elmer spectrum BX, averaging 100 scans with a nominal resolution of 4 cm^{-1}. The Raman spectra were measured using a Renishaw Raman imaging microscope system 2000, with laser excitation at 785 nm in the range between 100 and 4000 cm^{-1} (resolution 2 cm^{-1}). ^{27}Al NMR and ^{31}P NMR spectra were recorded at ambient temperature on Varian Mercury V-400 spectrometer using 7 mm CPMAS probes. The resonance frequencies were 162 and 149 MHz for ^{31}P and ^{27}Al, respectively.

Specific surface areas of the samples were determined by nitrogen adsorption at −196 °C using a Micromeritics ASAP 2000 equipment. Samples were previously degassed in situ at 120 °C under vacuum for 4 h. The surface area of the catalysts was calculated using the Brunauer–Emmet–Teller (BET) method over a p/p_0 range where linear relationship was maintained.

Morphological features of the HTlcs samples were studied using a scanning electron microscope (SEM, model: JEOL model JSM-6400). For the preparation of the samples for SEM, the powdered materials were first spread on sample buttons using conducting cement and then sputtered with gold. The acidity measurements were determined by the temperature programmed desorption (TPD) of NH_3, on a Thermo Finnigan TPDRO 1100 equipped with a TCD detector. Typically, ca. 0.200 g of sample were pretreated with Ar at 80 °C during 1 h and then cooled to room temperature and treated NH_3 flow (5% NH_3 in He). The desorption of NH_3 were measured heating the sample from room temperature to 700 °C and at heating rate of 10 °C/min in He flow (20 ml/min). The water

Table 1
Initial conditions and the composition of each synthesized sample.

Entry	HTlc	Synthesis conditions		Results of elementary analysis						
		pH	n (mmol)[a]	%Mg[b]	%Al[b]	%C[b]	%Cl[b]	%P[b]	%N[b]	x_{solid}[c]
1	HT-1	10	0.25	23.59	7.44	1.08	7.76	0.21	–	0.22
2	HT-2	10	0.50	23.97	7.54	1.21	5.47	0.13	–	0.22
3	HT-5	10	2.5	23.04	7.28	2.06	5.43	0.51	–	0.22
4	HT-6	10	5	22.85	7.19	1.83	7.74	1.21	–	0.22
5	HT-7	7	2.5	9.12	18.79	0.42	8.32	2.07	–	0.65
6	HT-8	7	5	12.5	15.26	0.62	3.53	3.26	–	0.52
7	HT-9a	10	5	23.9	7.59	0.17	–	1.32	2.26	0.22
8	HT-9b	10	7.5	24.2	7.67	0.15	–	1.99	1.76	0.22
9	HT-9c	10	10	22.3	7.11	0.19	–	2.71	1.92	0.22

[a] n is the initial quantity of phosphate ions in the solution.
[b] % in weight.
[c] Correspond to the molar ratio Al/Al + Mg.

was trapped on the corresponding drying agent, in order to avoid interferences. The number of acid sites was calculated from the TPD peaks by deconvolution using the software of the equipment, and a calibration of the instrument using known amounts of NH_3.

2.3. Catalyst evaluation: DMC synthesis from CO_2 and CH_3OH

MeOH (99.9% dried) was purchased from Aldrich and used without further purification. The continuous carboxylation of methanol was carried out in a continuous system formed of a tubular quartz packed-bed reactor (10 mm I.D.) and a furnace equipped with a temperature controller. The reaction was performed at temperatures between 100 °C and 200 °C. The methanol at 0 °C was bubbled by using helium carrier gas with a flow rate of 5 ml/min and introduced into the pre-heated reactor with 250 mg of phosphated Mg/Al mixed oxides catalyst. The CO_2 was also introduced into the reactor with a feed flow of 5 ml/min. The final molar ratio of CO_2/CH_3OH was 25. The final product was analyzed in a continuous form by a Shimadzu GC 17A gas chromatograph equipped with a capillary column (HP-Plot Q-divinyl benzene styrene polymer 1909 1P-Q04).

3. Results and discussion

The results of the elemental analysis of the synthesized HTlc compounds show that the materials prepared at a pH of 10 have an x_{solid} parameter, which is the molar ratio $Al^{3+}/(Al^{3+} + Mg^{2+})$, equal to 0.22 (entries 1–4 and 7–9, Table 1), whereas the materials prepared at pH 7 are enriched in aluminium content with an x_{solid} parameter above 0.5 (entries 5 and 6, Table 1). In the latter case, the octahedral of Al can form an excess of $Al(OH)_3$. The compensating anions in the interlayer space of the HTlcs demonstrate the effect of the salt precursors used in the synthesis. The samples prepared from the chloride salts present chloride, carbonate and phosphate species in the interlaminar space (entries 1–6, Table 1), whereas nitrates rather than chloride were present in the samples prepared using nitrate salts (entries 7–9, Table 1). Furthermore, the results of the elementary analysis of the samples HT-9a, HT-9b, HT-9c show that when the concentration of the Na_2HPO_4 solution used during the synthesis of the materials increases, the phosphate content in the HTlcs sample increases (entries 7–9, Table 1). Similar behaviour was observed in the materials synthesized from the chloride salts regardless of the pH used (entries 2, 3, 5 and 6, Table 1). The elementary analysis also shows that there is no correlation between the amounts of the carbonate species in the samples and the pH used during the co-precipitation. However, the kind of precursor salt used affects the amount of carbonate observed in the final material, so samples synthesized from nitrates salts contain only traces of CO_3^{2-}.

It is known that phosphate ions could exist in a monovalent ionic state ($H_2PO_4^-$), a divalent ionic state (HPO_4^{2-}) or a trivalent ionic state (PO_4^{3-}) according to the pH of the solution. The dissociation of orthophosphoric acid molecules (H_3PO_4) can be presented as the following equilibriums [13]:

$$H_3PO_{4(s)} + H_2O_{(l)} \leftrightarrows H_2PO_4{}^-{}_{(aq)} + H_3O^+{}_{(aq)} \quad pK_1 = 2.3 \tag{2}$$

$$H_2PO_4{}^-{}_{(aq)} + H_2O_{(aq)} \leftrightarrows HPO_4{}^{2-}{}_{(aq)} + H_3O^+{}_{(aq)} \quad pK_2 = 7.2 \tag{3}$$

$$HPO_4{}^{2-}{}_{(aq)} + H_2O_{(aq)} \leftrightarrows PO_4{}^{3-}{}_{(aq)} + H_3O^+{}_{(aq)} \quad pK_3 = 12.4 \tag{4}$$

According to the equilibrium observed at pH 7 (Eq. (3)) the composition of the phosphate ions is calculated to be 62% $H_2PO_4^-$ ions and 38% HPO_4^{2-} ions, whereas the composition in the phosphate ions in aqueous solution is about 100% HPO_4^{2-} ions according to the equilibrium at pH 10 (Eq. (4)). Consequently, the presence of different species of phosphates is strongly influenced by the pH during the synthetic process. Nevertheless, the phosphate specie intercalated in the aqueous medium can modify when the catalyst is dried.

Fig. 1a and b shows the XRD patterns of the synthesized samples at pH 10 in the presence of chloride and nitrate ions, respectively. These are in agreement with those reported in the literature on HTlcs [14,15]. All diffraction lines were identified in the hexagonal lattice with the rhombohedra symmetry $R\bar{3}m$ [ASTM Index No. 22-700]. The reticular distances d_{003} and d_{110} can be obtained from the most intense line and are indexed as (0 0 3) and (1 1 0), respectively [16]. The a parameter of the layered structure corresponds to the average cation–cation distance within the brucite-like layers. The c-parameter is related to the thickness of the brucite-like layer and the interlayer distance. The parameters are $a = b = 2d_{110} = 3.05$ Å and $c = 3d_{003} = 23.80$ Å for the samples in Fig. 1a [17].

These parameters allowed us to evaluate the extent to which the inter-lamellar distance depends on the size of the inserted anion and the amount of water molecules between the layers. The value of c observed in the synthesized catalysts is superior to that of Mg–Al–CO_3 HTlcs (22.9 Å) probably due to the insertion of phosphate ions. The XRD patterns of samples prepared at pH 7 are shown in Fig. 1c. They also agree with those reported in the literature on HTlcs [16,17]. They exhibit the broad and asymmetrical reflections for the (0 0 3) and (0 0 6) planes that are characteristic of a poor-crystallized HTlc phase. Furthermore, the values of the a parameter related to the solids HT-7 and HT-8 are equal to 3.01 Å, indicating that the value of a declines when x increases, in accordance with the Vegard law [18]. On the other hand, the elemental analysis (Table 1, entries 7–9) and the XRD characterization (Fig. 1a) of samples HT-9a, HT-9b and HT-9c prepared at pH 10 show a well-crystallized HTlc phase that contains significant quantities of phosphate in the interlayer space. Similar behaviour has been observed by Evans and Duan [1]. We focused our research on samples HT-9a, HT-9b

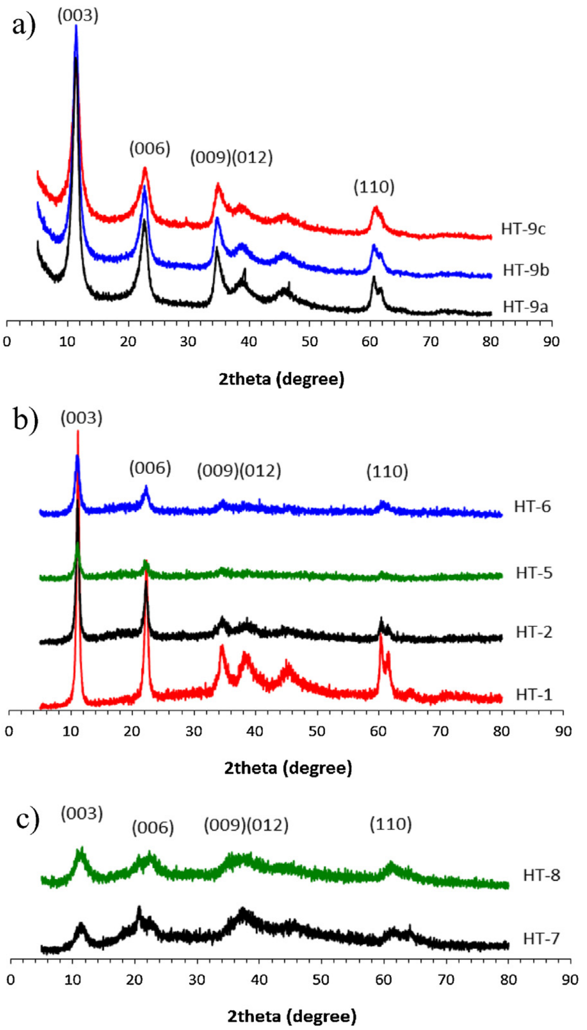

Fig. 1. XRD of the catalysts prepared by co-precipitation (a) at pH 10 for the samples in the present of nitrate anions, (b) at pH 10 in the present of chloride anions, (c) at pH 7 in the present of chloride anions.

Table 2
Surface area and textural parameters of calcined phosphated Mg/Al mixed oxides.

Catalyst	S_{BET} ($m^2 g^{-1}$)	Vp ($cm^3 g^{-1}$)	Dp (Å)
HT*c*-9a	54	0.36	316
HT*c*-9b	72	0.39	146
HT*c*-9c	85	0.38	91

and HT-9c to determine the nature of the phosphate ions retained in the interlayer space and their interactions with the HTlc layer. We decided to do this because of (i) the significant differences in crystallinity among the phosphoric acid intercalated Mg–Al HTlcs compounds synthesized at pH 10 with the chloride salt precursor and (ii) the significant difference in the amount of phosphates intercalated in these three samples.

The specific surface area and textural parameters of the calcined samples HT*c*-9a, HT*c*-9b and HT*c*-9c are reported in Table 2. It can be notice that, in general, the surface area of HT*c*-9a, HT*c*-9b and HT*c*-9c is lower than that corresponding to the non-phosphorous content calcined Mg/Al-HTs [19]. However, their specific surface area increases as increase the amount of phosphate species.

The IR spectra for the calcined samples HT*c*-9a, HT*c*-9b and HT*c*-9c are almost identical to those obtained for well known HTlc phases, Fig. 2.

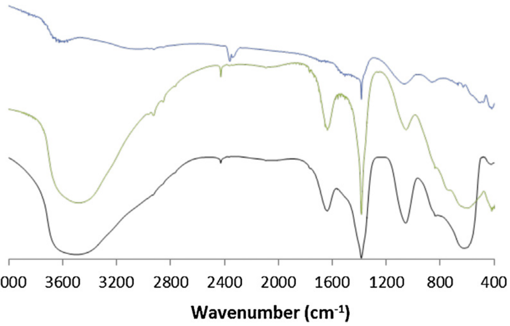

Fig. 2. FT-IR of the HT-9a, HT-9c and HT*c*-9c samples where the field of frequency varies between 400 and 4000 cm^{-1}.

The assignment of the main peaks from the IR spectrum corresponding to the HT-9c sample is communicated in Supporting Information (T1).

An averagely intense band situated at 1060 cm^{-1} can be attributed to the ν_3 asymmetric stretching vibration of the P—O bond [20]. Because of the pH of the solution, the HPO_4^{2-} ion is intercalated with nitrate ions in the interlayer of the HTlcs. However, the two shoulders at 1120 cm^{-1} and 990 cm^{-1} that are mentioned in literature regarding the vibration modes of HPO_4^{2-} are missing, and this is probably due to the low concentration of phosphorus or indicates a partial deprotonation during the intercalation. Upon heating at 400 °C, the water disappears due to the thermal decomposition of the HTlcs, and the band at 1635 cm^{-1} is not observed [21]. The bands at 1382 cm^{-1} and 827 cm^{-1} due to nitrates with symmetry D_{3h} are also present (Fig. 2, T1 in Supporting Information) while band at 1513–1528 cm^{-1} due to the C_{v2} symmetry is not observed. This fact does not fully agree with those reported by Evans and Duan [1] where some of the nitrate ions still retained in the interlayer space have been converted from D_{3h} to C_{2v} symmetry. The difference between our results and those presented by Evans et al. is probably caused by the presence of phosphate ions in our samples. Therefore, for this kind of sample the IR spectra do not differentiate unequivocally between C_{3v} and T_d phosphate symmetries. However, given the co-precipitation pH, C_{3v} symmetry is preferred. Thus, the presence of phosphate ions and nitrate ions in the interlayer space could induce thermal stability in the HTlcs.

In order to reach more reliable conclusions regarding spectra-structure, the Raman spectra of the synthesized HTlcs were recorded without and with phosphate ions (Fig. 3).

The assignments of the main peaks from the Raman spectrum corresponding to the HT-9c sample are indicated at Table T2 in Supporting Information.

A band at 960 cm^{-1} and a shoulder at 1050 cm^{-1} were observed, although only in the spectra of the HTlcs with phosphate ions. The shoulder was revealed by deconvolution of the band at 1044 cm^{-1} (Fig. 3b) and these bands were assigned to ν_1 symmetric and ν_3 anti-symmetric stretching vibrations of PO, respectively [22]. Although these HTlcs were synthesized at pH 10, the phosphate ions were intercalated as HPO_4^{2-}. Also, the Raman spectra for the calcined HTlcs HT*c*-9b and HT*c*-9c showed the same bands that were observed for the uncalcined samples (Fig. 3c). However, the bands at 960 and 1050 cm^{-1} shifted to 974 and 1089 cm^{-1}, respectively. This shift could be caused by a decrease in hydrogen bonds between the uncalcined and calcined HTlcs. Also, a shift from 1044 to 1048 cm^{-1} was observed in the symmetric vibrational band of NO_3^-.

Also, detailed solid state NMR experiments are used to reveal the relevant species present in these materials.

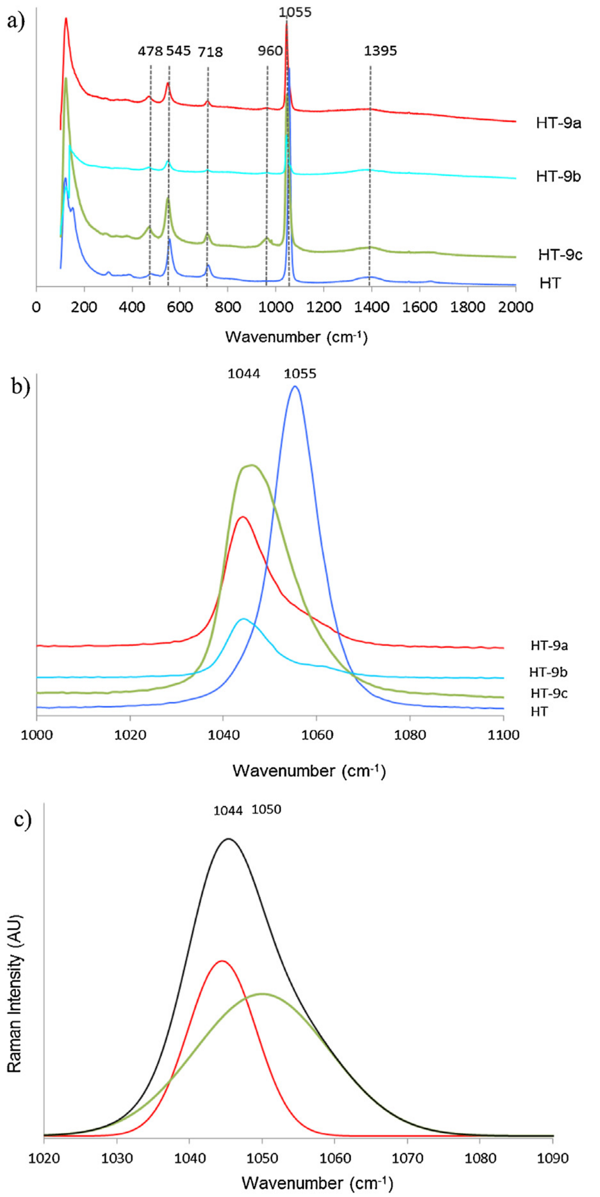

Fig. 3. (a) Raman spectra of HT, HT-9a, HT-9b and HT-9c between 100 and 2000 cm^{-1}, (b) Raman spectra between 1000 and 1100 cm^{-1} of HT, HT-9a, HT-9b and HT-9c, (c) deconvolution of the bands at 1044 cm^{-1} and 1050 cm^{-1} from HT-9a.

^{27}Al MAS NMR spectra (Fig. S1 in Supporting Information) consist of a symmetric series of spinning side bands and the signals from the solids. The spectra for the uncalcined HTlcs have a peak around 4.5 ppm for HT-9c, a peak around 9.5 ppm for HT-9b and HT-9a, and a peak of very low intensity around 102–104 ppm. Nevertheless the spectrum for the calcined sample also exhibited a very low signal at 80 ppm. The peak at 4.5–9.5 ppm is assigned to the aluminium atoms in the octahedral site of AlO_6 in the sheet of HTlcs. The peak at 80 ppm represents the tetrahedral coordination of aluminium in a network type AlO_4. Assignments for these peaks are well established in the literature [23–25]. These results confirm that most of the aluminium occupies an octahedral site and is mostly preserved in the calcined samples. The peak at 102–104 ppm that is present in all the ^{27}Al MAS NMR spectra of our samples could be attributed to an aluminium atom in a type AlO_3 network that seems not be modified after the calcination.

The ^{31}P MAS NMR spectrum for the uncalcined HTlcs (HT-9c) (Fig. S2 in Supporting Information) exhibited two signals, an intense peak centred at −22.3 ppm and a second at 14.5 ppm, whereas, the spectrum of calcined HTlcs (HT*c*-9c) only showed a single peak at −25 ppm and a symmetric series of spinning side bands. In conjunction with the literature [26], these resonances at −22.3 ppm and at −25 ppm are most probably attributable to the fact that orthophosphate species have three Al neighbouring cations occupying octahedral sites ($OP(O{-}Al)_3$). It should be noted that due to the intensity of the signals, most of the phosphorus is in this form. The less intense resonance peak of the phosphorus atom (14.5 ppm), can be assigned to tetrahedral $O_3P(O{-}H)$ on the basis of its downfield shift. This peak is not present in the HT*c*-9c due to dehydration and partial dehydroxylation of the synthetic precursor HT-9c compound. This result shows that only a very small amount of phosphorus has a PO—H bond in the orthophosphate form ($O_3PO{-}H$) where the oxygen atoms can be bonded to a metal (Al or Mg) in the HTlcs layer. Furthermore, together with the ^{27}Al MAS NMR peak at 103 ppm in the HT*c*-9c sample suggests the presence of $(AlO_3PO{-}H)^+$ like-species on the surface of the HTlcs.

The acidity of the calcined HTs was measured by TPD-NH_3. The acid strength could be assigned according to the temperature at which peaks appeared, where the number of basic sites was estimated by integration of these peaks (Table 3, Fig. 4).

HT*c*-9cUS corresponds to the HT*c*-9c sample which was treated back in decarbonated water by sonication for 1 h under an inert atmosphere to maximize the accessibility of the phosphates species. The NH_3-TPD profiles for these samples have showed broad profiles extended from 100 to 500 °C which were deconvoluted in three desorption peaks with maxima in the ranges 200–220 °C, 260–285 °C and 330–360 °C corresponding to weak, medium and strong acid sites, respectively. The total number of accessible acid sites, particularly the medium and strong sites increase by ultrasonic activation, entries 1 and 2, Table 3.

Fig. S3 in Supporting Information displays the electron micrographs of the calcined synthesized materials. The micrographs were obtained using SEM at 50,000× magnifications. The shape of the HT-9a particles seems slightly irregular in comparison to the regular hexagonal platelet structure characteristic for Mg/Al-HTs particles. The regularity of the HT-9a particles confirmed the crystallinity evidenced by X-ray measurement. The thickness of these platelet-stacks is around few hundred nanometers and the lateral dimension is in the range of 1–2 μm. In the case of the calcined samples (HT*c*-9a, HT*c*-9b and HT*c*-9c), the morphological features are different that to parent non calcined HTs and gives evidence of loss of hexagonal platelet HTs morphology which is most evident in the sample with higher amount of P (HT*c*-9c). This is probably due to the effect of the orthophosphate specie present in the HTs. In addition, the no presence of conglomerate on the surface of the HT*c*-9c and the homogeneous distribution of the phosphorous atom in the material indicate the interlayer arrangement of the orthophosphate species.

Because of their physical-chemical and textural characteristics, the HT*c*-9c sample was tested in a catalytic direct carboxylation reaction of methanol in gas phase in a continuous reactor. The results obtained were compared with the calcined at 450 °C hydrotalcite with Mg/Al molar ratio of 3:1 (HTO). Table 4 shows, in terms of conversion from methanol (%Conv.) and selectivity to DMC (%S), the results of using HT*c*-9c (0.250 g) as a catalyst in the continuous carboxylation reaction with a MeOH:CO_2 molar ratio of 25. DME was also obtained as a side product. The DME could be generated by two different catalytic processes: (i) the intermolecular dehydration of the MeOH [27] and the thermal decomposition of the DMC [28]. Recently, it has been showed that the decomposition of DMC is the principal side reaction of the carboxylation reaction catalyzed by HTOs supported onto lyogels at moderate temperatures [29].

Table 3
Number of acid sites of different strength for phosphated Mg/Al mixed oxides, derived from TPD of NH_3.

Catalyst	Number of acid sites (μmol g^{-1})			Total number (μmol g^{-1})
	Weak (%)	Medium (%)	Strong (%)	
HT*c*-9c	49.3 (40.2)	33.4 (27.2)	39.3 (32.6)	122.5
HT*c*-9cUS	40.2 (27.2)	46.7 (31.7)	60.7 (41.1)	147.6
HT*c*-9c tested	52.6 (41.7)	36.4 (28.8)	37.2 (29.5)	126.3

The effect of the temperature was studied in the carboxylation reaction of MeOH with the HT*c*-9c catalyst (Table 4). The reaction showed that DME was almost the only product working at more than 200 °C and that conversion was very low at temperatures below 150 °C (Table 4, entries 3 and 6). The reaction at 200 °C provided higher conversion (16%) than at 175 °C (2.6%) (Table 4, entries 4 and 5). The selectivity towards DMC was very sensitive to temperature. Whereas the carboxylation reaction at 150 °C has showed full selectivity to DMC, the increases in the reaction temperature (175 °C) resulted in lower selectivity to DMC (57.8%).

Table 4
Catalytic carboxylation reaction of MeOH.

Entry[a]	Catalyst	*T* (°C)	%Conv.[c]	%S[c]
1	HTO	150	1.8	99.9
2	HTO	175	2.5	39.7
3	HT*c*-9c	120	0.2[b]	N.D.
4	HT*c*-9c	150	2.2	99.9
5	HT*c*-9c	175	2.6	57.8
6	HT*c*-9c	200	16.0	13.5
7	HT*c*-9cUS	150	2.3	99.9

[a] Standard catalytic conditions: the methanol at 0 °C was bubbled by using helium carrier gas with a flow rate of 5 ml/min, 250 mg of phosphated Mg/Al mixed oxides catalyst, CO_2 feed flow of 5 ml/min, molar ratio of CO_2/CH_3OH was 25; 30 min of reaction time. %Conv. means total conversion from methanol where the unique products observed were the DMC and the DME. %S means selectivity towards DMC. N.D. means non-determined.
The unique products observed where

[b] Almost not conversion, the value was calculated by extrapolation of the calibration curve but out of the limit of quantification.

[c] The final product was analyzed in a continuous form by a Shimadzu GC 17A gas chromatograph equipped with a capillary column (HP-Plot Q-divinyl benzene styrene polymer 1909 1P-Q04).

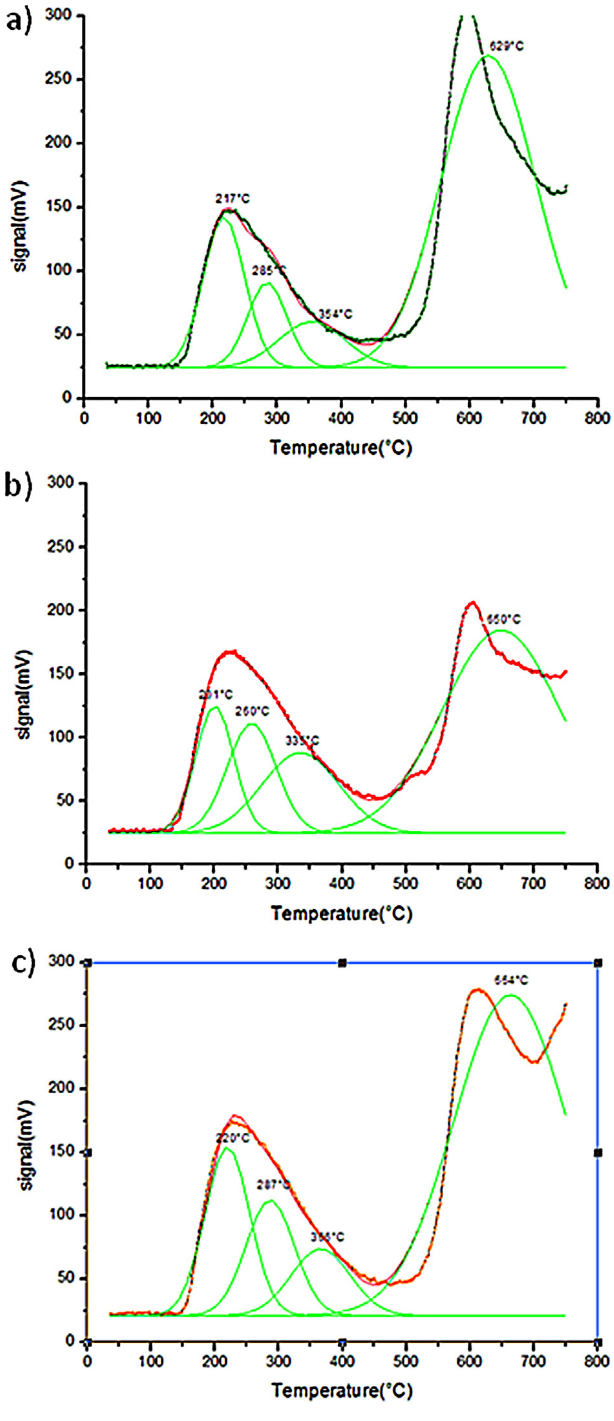

Fig. 4. TPD-NH_3 profile of (a) HT*c*-9c, (b) HT*c*-9cUS, (c) HT*c*-9cUS tested.

The mixed Mg–Al oxides (HTO) derived from hydrotalcite without the incorporation of phosphates species in the interlayer space are known to exhibit both weak acidic and weak basic properties [30]. However, the HT*c*-9c (P/Mg molar ratio = 0.11) catalyst showed slightly higher conversions and higher selectivities towards DMC than the HTO (Table 4, entries 2 and 5). These results show that the decomposition of DMC is a less-favoured process in the presence of ortophosphonate based catalyst. Ikeda et al. suggest that activating CO_2 on base sites leads to methyl carbonate species and that is an intermediate reaction [31]. Also, activating CH_3OH on the acid sites allowed the formation of a methyl cation which reacts with the methyl carbonate to form DMC. In addition, they show that the presence of Brønsted acid sites are more favourable than the Lewis acid sites for this activation. In this context, the presence of orthophosphates changes the acid properties of the material, specially via the activation of Al^{3+} by the formation of $(AlO_3PO—H)^+$. This illustrates the presence of Brønsted acid sites which are located near the P atoms and promotes the interaction between CH_3OH and Al^{3+} in the carboxylation reaction and, at the same time, decreases the decomposition of DMC.

In order to increase the accessibility of the acid and basic sites, the calcined HT*c*-9cUS (where the HT*c*-9c was rehydrated under ultrasounds for 1 h in the presence of decarbonated water and then calcined at 450 °C) was tested as a catalyst in the carboxylation reaction of MeOH. As a result, the conversion increased slightly to 2.3% and the selectivity was almost complete which indicates the high stability of the catalyst with orthophosphate content.

HT*c*-9cUS after catalytic test was analyzed by NH_3-TPD, entry 3, Table 3. The strong acid centres and the total number of acid sites decreased after the catalytic test.

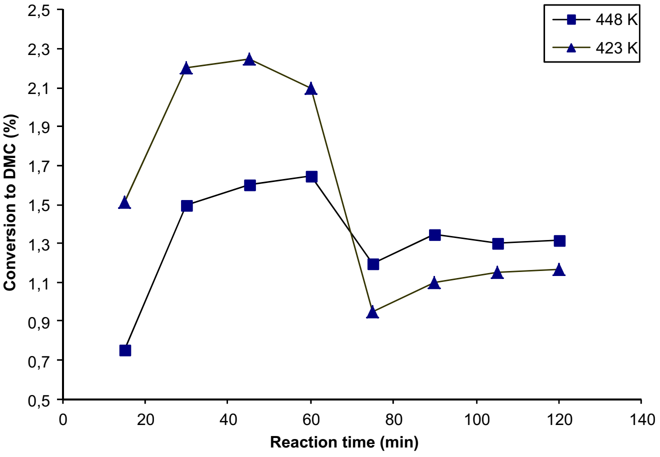

Fig. 5. Study of the stability of HT*c*-9c catalyst at different temperatures (448 K and 423 K) in the carboxylation reaction of MeOH. The methanol at 0 °C was bubbled by using helium carrier gas with a flow rate of 5 ml/min, 250 mg of phosphated Mg/Al mixed oxides catalyst, CO_2 feed flow of 5 ml/min, molar ratio of CO_2/CH_3OH was 25. The final product was analyzed in a continuous form by a Shimadzu GC 17A gas chromatograph equipped with a capillary column (HP-Plot Q-divinyl benzene styrene polymer 1909 1P-Q04).

Fig. 5 shows how the activity of the HT*c*-9c catalyst decreases significantly after 1 h of reactions at 150 °C and 175 °C. However, it seems that the catalyst deactivation is softer when the reaction is performed at higher temperature. This behaviour could be explained by the irreversible chemisorptions of the CO_2 in the basic centres at low temperatures.

4. Conclusions

The synthesis of hydrotalcite phase with phosphate ions in the interlayer space is achieved by a co-precipitation method that involves a low supersaturation. The molar ratio Al/(Al + Mg) of the initial solution (0.22) is almost entirely preserved in the solid form when the pH of the solution equals 10. At pH 7 the Al/(Al + Mg) ratio increases to 0.65 but the solid form is not a pure hydrotalcite phase. FT-IR, Raman, ^{31}P and ^{27}Al MAS NMR spectroscopies were used to investigate phosphate ions in the hydrotalcite phase. The correlation between the results shows that the phosphate is intercalated mainly in the form of PO_4^{3-} that is linked to the Al^{3+} ions which occupy octahedral sites in the layers, whereas a very small amount of HPO_4^{2-} ion is extracted by the Al^{3+} ions, which suggests $(AlO_3PO{-}H)^+$ species on the surface of the solid. Thus the strong interaction between the phosphate ions retained in the interlayer space and the ions in the aluminium sheet decreases the distance between the layers to $d_{003} = 7.93$ Å (value measured by XRD) and gives thermal stability to the HTlcs.

Due to the acid-basic characteristic of the synthesized solids, we investigated the catalytic performance of the well-crystallized HTlc HT-9c activated by calcination (HT*c*-9c) during the synthesis of DMC from MeOH and CO_2. The catalytic activity observed at low temperatures was significantly higher than the 1%Conv. reported in the literature for heterogeneous catalysts. On the other hand, the selectivity of the HT*c*-9c and HTO was highly dependent on the temperature because of the formation of DME as a side product mainly due to the decomposition of DMC. Nevertheless, the presence of orthophosphate in the catalytic structure of the HTO reduces the conversion towards the side product (DME) increasing significantly the selectivity of the carboxylation process.

The experimental results show that the type of acidic centre has a large influence on the activity in the heterogeneous carboxylation reaction. In addition, the phosphate species favours the Brønsted acid sites on Mg/Al catalyst and promotes the carboxylation reaction of the methanol in gas phase.

Even if improvement of activity remains necessary, the in-depth characterization of the HTs with orthophosphates content, together with the catalytic results should be significant in understanding and designing heterogeneous catalysts for the carboxylation reaction.

Acknowledgements

Authors acknowledge the financial support from the Spanish Government's Ministry of Science and Technology, as part of a Research draft inter-university Tunisian-Spanish achieved during the period January 2012–June 2013 (Project CTQ2006-08196 and AP/037098/11).

Appendix A. Supplementary data

Supplementary data associated with this article can be found, in the online version, at http://dx.doi.org/10.1016/j.apcata.2015.01.004.

References

[1] D.G. Evans, X. Duan, Mater. Chem. Phys. 85 (2004) 207–214.
[2] X. Duan, D.G. Evans (Eds.), Layered Double Hydroxides, Springer, Germany, 2006.
[3] A. Ookubo, K. Ooi, H. Hayashi, Langmuir 9 (1993) 1418–1422.
[4] A. Ookubo, K. Ooi, F. Tani, H. Hayashi, Langmuir 10 (1994) 407–411.
[5] J. Das, B.S. Patra, N. Baliarsingh, K.M. Parida, Appl. Clay Sci. 32 (2006) 252–260.
[6] X. Cheng, X. Huang, X. Wang, D. Sun, J. Hazard. Mater. 177 (2010) 516–523.
[7] K.M. Parida, S. Parija, J. Das, P.S. Mukherhee, Catal. Commun. 7 (2006) 913–919.
[8] Y. Ono, Appl. Catal. A 155 (1997) 133–166.
[9] J. Hagen, Industrial Catalysis: A Practical Approach, second ed., Wiley-CH Verag GmbH and C. KGaA, Weinheim, 2006.
[10] Y. Yoshida, Y. Arai, S. Kado, K. Kunimori, K. Tomishige, Catal. Today 115 (2006) 95–101.
[11] K. Tomishige, Y. Ikeda, T. Salairhori, K. Fujimoto, J. Catal. 192 (2000) 355–362.
[12] M. Aresta, E. Quaranta, Chem. Tech. 27 (1997) 32–40.
[13] D. Perrin, D.B. Dempsey, Buffer for pH and Metal Ion Control, Chapman and Hall, London, 1974, pp. 156, 159 and 162.
[14] R. Allman, Acta Crystallogr. B 27 (1968) 972–977.
[15] H.F.W. Taylor, Mineral. Mag. 37 (1969) 338–342.
[16] F. Cavani, F. Trifiro, A. Vaccari, Catal. Today 11 (1991) 173–301.
[17] Z.P. Xu, H.C. Zeng, J. Phys. Chem. B 105 (2001) 1743–1749.
[18] C.J. Brinker, G.W. Sherer, Sol-Gel Science, Academic Press, New York, 1989.
[19] D. Tichit, M. Naciri Bennani, F. Figueras, R. Tessier, J. Kervennal, Appl. Clay Sci. 406 (1998) 401–415.
[20] R.L. Frost, Spectrochim. Acta A 60 (2004) 1439–1445.
[21] J.T. Kloprogge, R.L. Frost, in: V. Rive (Ed.), Infrared and Raman Spectroscopic Studies of Layered Double Hydroxides: Present and Future, Nova Science Publishers, Inc., New York, 2001.
[22] R.L. Frost, A.W. Musumeci, J.T. Kloprogge, M.O. Adebajo, W.N. Martens, J. Raman Spectrosc. 37 (2006) 733–741.
[23] T.J. Park, S.S. Choi, Y. Kim., Bull. Korean Chem. Soc. 30 (2009) 149–157.
[24] A. Vyalikh, D. Massiot, U. Scheler, Solid State Nucl. Magn. Reson. 36 (2009) 19–23.
[25] L. Zhang, Phosphorus Res. Bull. 15 (2004) 177–185.
[26] M. Hartmann, A.M. Prakash, L. Kevan, J. Chem. Soc., Faraday Trans. 94 (1998) 723–727.
[27] X.L. Wu, M. Xiao, Y.Z. Meng, Y.X. Lu, J. Mol. Catal. A: Chem. 238 (2005) 158–162.
[28] Y. Fu, H. Zhy, J. Shen, Thermochim. Acta 434 (2005) 3972–3978.
[29] S. Dragos, E. Taboada, J. Llorca, E. Molins, F. Medina, A.M. Segarra, Chem. commun. 49 (2013) 5489–5492.
[30] M. Asadullah, K. Fujimoto, K. Tomishige, J. Phys. Chem. B 105 (2001) 10653–10658.
[31] K. Tomishige, Y. Ikeda, T. Sakaihori, K. Fujimoto, J. Catal. 192 (2000) 355–362.